UNIVERSITY OF LEEDS

Article:
Bradley, D, Lawes, M orcid.org/0000-0002-8693-7536, Mumby, R et al. (1 more author) (2019) The stability of laminar explosion flames. Proceedings of the Combustion Institute, 37 (2). pp. 1807-1813. ISSN 1540-7489

https://doi.org/10.1016/j.proci.2018.07.067

The Stability of Laminar Explosion Flames

Bradley, D., Lawes, M.*, Mumby R., Pervez Ahmed

University of Leeds, School of Mechanical Engineering, Leeds LS2 9JT, UK.

*Corresponding author email: m.lawes@leeds.ac.uk

Colloquium:

1. LAMINAR FLAMES
2. DETONATIONS, EXPLOSIONS, AND SUPERSONIC COMBUSTION

Total length of the paper: 6173.7

Method 1

Word Equivalent

Main Text = 2907

Nomenclature = (17 lines + 4 lines) x (7.6 words/line) = 169.6

References = (27 references + 2) x (2.3 lines/reference) x (7.6 words/line) = 506.9

Figure 1 = (85 mm + 10 mm) x (2.2 words/mm) x (2) + (26) = 444

Figure 2 = (60 mm + 10 mm) x (2.2 words/mm) x (2) + (10) = 318

Figure 3 = (120 mm + 10 mm) x (2.2 words/mm) x (2) + (14) = 586

Figure 4 = (85 mm + 10 mm) x (2.2 words/mm) x (2) + (24) = 442

Figure 5 = (85 mm + 10 mm) x (2.2 words/mm) x (2) + (25) = 443

Table 1 = (10 lines + 2 lines) x (7.6 words/line) x (2) = 182.4

Equations = (9 eqn lines + 14 blank lines) x (7.6 words/line) x (1) = 174.8

List of figure captions

Figure 1: Pe_{cl} variations with Ma_b for different hydrocarbons and H_2 [19] at 0.1 MPa in the explosion vessel with data from large scale explosions [7-9].

Figure 2: Pe_{cl} variations with Ma_b for different hydrocarbon/air explosion vessel data.

Figure 3: Values of K_{cl} plotted against Ma_{sr} for all hydrocarbon/air explosion vessel data.

Figure 4: K_{cl} variation with Ma_{sr}. Explosion vessel data for different hydrocarbon/air mixtures at different pressures. Crosses (0.1 MPa), open circles (0.5 MPa), filled squares (1.0 MPa). Solid curves shows best fits through these data.

Figure 5: Solid curves show K_{cl} variations with Ma_{sr} from explosion vessel data at 0.1, 0.5 and 1.0 MPa alongside data for LS atmospheric explosions [7-9].

Abstract

The paper presents the results of a fundamental experimental and theoretical study of Darrieus-Landau, thermo-diffusive, instabilities in atmospheric explosions, and, on a smaller scale, in laboratory explosions in closed vessels. Pressure dependencies were sought to exploit the leading role of the Peclet number in the phenomena, so that similar Peclet numbers were achieved in both instances. However, in the large atmospheric explosions a large Peclet number was achieved by the distance scale of the fireball, whereas in the closed vessel explosion it was achieved at a higher pressure by a much smaller flame, but because of the higher pressure, one endowed with a small laminar flame thickness. This study covers a much wider range of fuels and of pressures and the dependencies of the phenomena on both of these were carefully studied, although, for the atmospheric explosions, the data only covered propane and methane. The roles of both Markstein and Peclet numbers become clear and give rise to a more fundamental correlating parameter, a critical Karlovitz number, K_{cl}, for flame stability. This is based on the flame stretch rate, normalised by its muliplication by the chemical reaction time in a laminar flame. The experimetnally measured dependencies of this key parameter on pressure and Markstein number are reported for the first time for so many different fuels. The critical Karlovitz number for flame stability decreases with increase in the strain rate Markstein number. As a result, it is possible to predict the extent of the unstable regime for laminar flames as a function of Ma_{sr} and pressure. Such data can be used to estimate the severity of large scale atmospheric explosions. As Ma_{sr} becomes highly negative, the regime of stability is markedly reduced.

Keywords: Darrieus Landau, thermo-diffusive instabilities, large-scale explosions, critical Peclet number, critical Karlovitz number.

Nomenclature

C_p	mass based specific heat at constant pressure (J/kg/K)
K_{cl}	critical Karlovitz number, ($\alpha_{cl}\,\delta_l/u_l$)
K	turbulent Karlovitz stretch factor
L_b	burned gas Markstein length (m)
Ma_b	flame speed Markstein number
Ma_{sr}	burning velocity strain rate Markstein number
P_a	atmospheric pressure (Pa)
Pe_{cl}	critical Peclet number
Pr	($C_p\eta/k$), Prandtl number
r_u	flame radius (m)
r_{cl}	critical flame radius (m)
S_n	stretched flame speed (m/s)
S_s	unstretched flame speed (m/s)
t	time (s)
u_l	unstretched laminar burning velocity (m/s)
u_n	stretched laminar burning velocity (m/s)

Greek

α	flame stretch rate (1/s)
δ_l	laminar flame thickness (m), $(\nu/u_l)/Pr$
η	viscosity (N.s/m^2)
k	thermal conductivity (W/m/K)
ν	kinematic viscosity (m^2/s)
ρ_b	density of burned gas (kg/m^3)
ρ_u	density of unburned gas (kg/m^3)
σ	unburned to burned gas density ratio
ϕ	equivalence ratio

Subscripts

b	burned
cl	critical
sr	strain rate
u	unburned

1. Introduction

A preliminary feasibility study [1] suggested Peclet number equalities at the onset of flame instabilities in explosions in laboratory closed vessels, and much larger ones in the atmosphere, might enable the former to predict the latter. The present paper reports an extension of this work over greater range of fuels and closed vessel pressures. Data for the large atmospheric explosions were drawn from the same sources in both studies. The flame stretch rate decreases as the flame propagates, and when it falls below a certain threshold, the interactions of the Darrieus Landau and thermo-diffusive instabilities create increasingly severe wrinkling of the initially smooth laminar flame surface, accelerating the flame speed and strengthening the associated pressure pulse, that arises from the rate of change of the heat release rate [2].

An important question is whether the wrinkled flame acceleration might lead to a detonation. The mathematically modelling of the increasing wrinkling of the flame surface, and the increasing flame speed present a severe challenge. Complete numerical simulations have only been possible up to a radius of a few cm. Consequently, semi-theoretical studies have involved a combination of fractal analyses [3,4] and experiments [5,6], some of which, in larger atmospheric explosions, have involved flame sizes of several metres [7-9]. Sivasinsky and co-workers [10,11] have developed a mathematical technique that involves multiplying the reaction rate with a degree of folding of the wrinkled flame front.

A key parameter is the critical flame radius, r_{cl}, that marks the onset of the unstable flame, with developing cellularity and an increasing flame speed, S_n. The appropriate dimensionless radius is the Peclet number, Pe_{cl}, comprised of r_{cl}, normalised by the laminar flame thickness, δ_l.

The theoretical approach in [12] expresses the growth rate of the amplitude of the flame front perturbation, A(n), for a given wave number, n, as:

$$A(n) = \omega\left(1 - (Pe_{cl}/Pe)\right). \qquad (1)$$

Pe, the general Peclet number, is the flame radius, r_u, normalised by δ_l, and ω is a perturbation growth rate parameter that depends upon n. As the flame grows, with $Pe < Pe_{cl}$, A(n) is negative, the amplitude diminishes, and the flame is stable. When $Pe > Pe_{cl}$, the sign becomes positive and the flame becomes unstable. The relative contributions of the Darrieus Landau and thermal diffusive instabilities to A(n) are in the ratio (Pe_{cl}/Pe). The

flame stability is increased by increases in strain rate Markstein number, Ma_{sr}, and σ, the ratio of unburned to burned gas density. The flame thickness is given by:

$$\delta_l = (\nu/u_l)/\mathrm{Pr}, \qquad (2)$$

where ν is the kinematic viscosity, u_l the unstretched laminar burning velocity, and $\mathrm{Pr} = C_p\eta/k$, the Prandtl number.

Theoretical [4, 12] and experimental [5, 13] studies have revealed the strong dependency of Pe_{cl} upon Ma_{sr}. The present paper reports measurements of Pe_{cl} for fuel/air mixtures in spherical explosions. Nine different fuels are studied at different equivalence ratios, ϕ, and pressures of 0.1, 0.5, and 1.0 MPa. Maximum generality is sought for these measurements, on the basis of theoretical studies.

The creation of cells only occurs when the localised flame stretch rate at the cell surface is sufficiently reduced to allow the growth of an instability of shorter wavelength. The onset of cell formation at Pe_{cl}, provides the limiting stretch rate, below which flame wrinkling occurs. The critical Peclet number is a convenient measure for the onset of instability, and is associated with the flame stretch rate, α_{cl}, multiplied by the chemical time, (δ_l/u_l), yielding a critical Karlovitz number, K_{cl}. For a spherical premixed laminar flame, this is expressed by [13] :

$$K_{cl} = (2\sigma/Pe_{cl})[1 + (2Ma_b/Pe_{cl})]^{-1}. \qquad (3)$$

Here Ma_b is the flame speed Markstein number, like Pe_{cl}, readily measurable. At normalised stretch rates below K_{cl}, the flame becomes unstable.

Experimental results are first presented by Pe_{cl} as a function of Ma_b then, because of the fundamental importance of the strain rate, K_{cl} is expressed as a function of the strain rate Markstein number, Ma_{sr} as in [13]. This parameter was obtained by determining the strain rate Markstein length, L_{sr}, from the associated flame stretch rate, α, and stretch burning velocity, u_n, using multiple regression analysis, [16]. The strain rate Markstein length, L_{sr}, divided by the laminar flame thickness, δ_l, yields Ma_{sr}. Experimental data are also drawn from large atmospheric explosions.

Values of K_{cl} and Ma_{sr} were measured for different fuels in an explosion vessel, at higher pressures than atmospheric, where the reduced value of δ_l yielded higher values of Pe_{cl}, simulating atmospheric explosions

with higher radii. Such generalised findings provide a means of predicting values of r_{cl} and S_n in larger atmospheric explosions, on the basis of small scale laboratory explosions. Another objective is to ascertain the extent to which K_{cl}/Ma_{sr} relationships might cover a wide range of fuels. Values of Pe_{cl} would then be found from Eq. (3), while the K_{cl}/Ma_{sr} relationship would define the regime of laminar flame instability.

2. Experimental Technique

Spherical flame propagations were measured in a spherical stainless steel explosion vessel with three pairs of orthogonal windows of 150 mm diameter [5,13]. The internal radius of the bomb was 190 mm. This provided a field of view of the constant pressure combustion, to observe the critical flame leading edges at the onset of instabilities and their subsequent development. The bomb and mixture could be heated and gas temperature measured with a sheathed chromel–alumel thermocouple. Four fans, driven by electric motors, located close to the wall of the bomb mixed the reactants. With liquid fuels, it was vital to ensure all the liquid was evaporated. The fans enhanced heat transfer and promoted mixing.

Flame speeds, together with the critical radii, r_{cl}, were measured for a variety of fuel/air mixtures, with the nine fuels listed in Table 1, using high speed ciné imaging. Measurements were taken at pressures of 0.1, 0.5 and 1.0 MPa and 360 K. Table 1 lists all the fuels, along with their equivalence ratios, ϕ, and references for data taken from other sources.The onset of flame cellularity and increasing flame speed are indicative of the onset of Darrieus Landau, thermo-diffusive instabilities. The flame speeds, $S_n = dr_u/dt$, changed with the leading radius of the flame front, r_u, due to the changing flame stretch rate, given by $\alpha = (2/r_u)(dr_u/dt)$.

Table 1: Experimental data sources

Apparatus	Mixture properties				Ref
	Fuel	T (K)	P (MPa)	ϕ	
Explosion vessel	H_2	365	0.1	0.3-1.0	[19]
Explosion vessel	CH_4	300-400	0.5-1.0	0.8-1.2	[6]
Explosion vessel	ethanol	358	0.5-1.4	0.8-1.4	[13]
Large Scale (LS)	CH_4, C_3H_8		0.1	0.81-1.22	[8][9]
Large vented box	CH_4, C_3H_8		0.1	1.1, 1.06	[7]
Explosion vessel	iso-octane, ethanol, n-heptane, toluene, C_3H_8, 1-hexene, n-butanol	360	0.1-1.0	0.8-1.3	Present work

Measurement extended from when the flame became established to the onset of instabilities. Within it, the flame speed, S_n, depends upon α and the flame speed Markstein length, L_b, in:

$S_s - S_n = L_b \alpha$. (4)

The S_n/α relationship, extrapolated to $\alpha = 0$, yielded an imaginary, notional, flame speed at zero stretch rate, S_s the "unstretched laminar flame speed." The laminar burning velocity is obtained by dividing this value by σ. The S_n/α relationship became more linear with increasing pressure.

The critical radius, r_{cl}, was measured where an upturn was first evident in the plot of S_n against α. The length, L_b, and radius r_{cl} were both normalised by δ_l, to yield the flame speed Markstein number Ma_b, and, Pe_{cl}, respectively. Fuller details are provided in [5,13]. Values of σ and ν were obtained using GasEq [14].

3. Experimental Results

Measured values of Pe_{cl}, for the listed hydrocarbons at pressures of 0.1, 0.5, 1.0 MPa, are plotted against measured values of Ma_b in Figs. 1 and 2, respectively. Each experimental point gives the mean value from three explosions. Values of ϕ ranged from 0.7 to 1.4 for propane-air mixtures, and from 0.8 to 1.2 for methane. For other hydrocarbons, values of fuels were limited to 0.8-1.3, due to limitations imposed by liquid vapour pressures. Asterisk symbols show values for hydrogen from [19] and the thin line curve shows the best fit. To obtain Ma_b for these H_2 data, values of L_b were taken from [23]. Data from much larger scale atmospheric explosions are also presented [7-9].

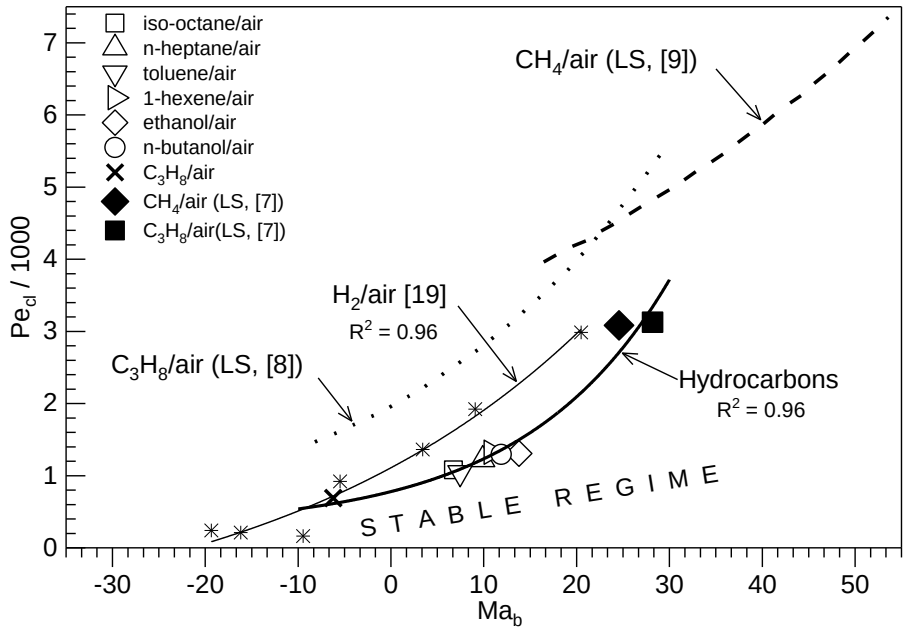

Figure 1: Pe_{cl} variations with Ma_b for different hydrocarbons and H_2 [19] at 0.1 MPa in the explosion vessel with data from large scale explosions [7-9].

The bold black diamond (methane) and black square (propane) data points in Fig. 1 are from large scale, LS, atmospheric explosions by Shell Research Ltd. in a large vented steel box structure, 10 m, long, 8.75 m wide and 6.25 m high [7]. Flame speeds were measured up to a radius of 3.5 m for CH_4/air, ϕ = 1.1, and C_3H_8/air, ϕ = 1.06.

Values of Pe_{cl} have been measured by the Factory Mutual group for, LS, atmospheric explosions, in [8] for C_3H_8/air flames, and in [9] for CH_4/air. Flames were up to 2 m diameter, with ϕ ranging between 0.81-1.22. These values are plotted against values of Markstein numbers, from [15]. These were numerically closer to the burning velocity strain rate Markstein numbers, Ma_{sr}, than the flame speed Markstein numbers, Ma_b [16]. To compare these values from [8] and [9] more closely with those in the present study, it was assumed they were those of Ma_{sr}. They were converted to Ma_b using the tabulated values of the different Markstein numbers in [6] for CH_4, and in [17] for C_3H_8. The correlated data from [8] and [9] then yielded the upper broken curves, in Fig 1. The dotted curve represents C_3H_8 results and the dashed curve those for CH_4.

Differences between Shell and Factory Mutual LS data are attributed to confusingly varied ways of defining Markstein numbers in different texts. Errors in the measurement of Ma_b are also important [15]. Other errors might arise from different ways in measuring r_{cl}. This is particularly so at negative values of Ma_b, where stable combustion is of short duration [18], and a fractal expression might be required for the extrapolation to zero stretch rate [19]. In addition, there are different interpretations of Markstein number, not only between Ma_b and Ma_{sr}, but also between different expressions for the latter [15, 16].

Figures 2a and 2b show plots of Pe_{cl} against Ma_b for different hydrocarbons, measured at 0.5 and 1.0 MPa, respectively.

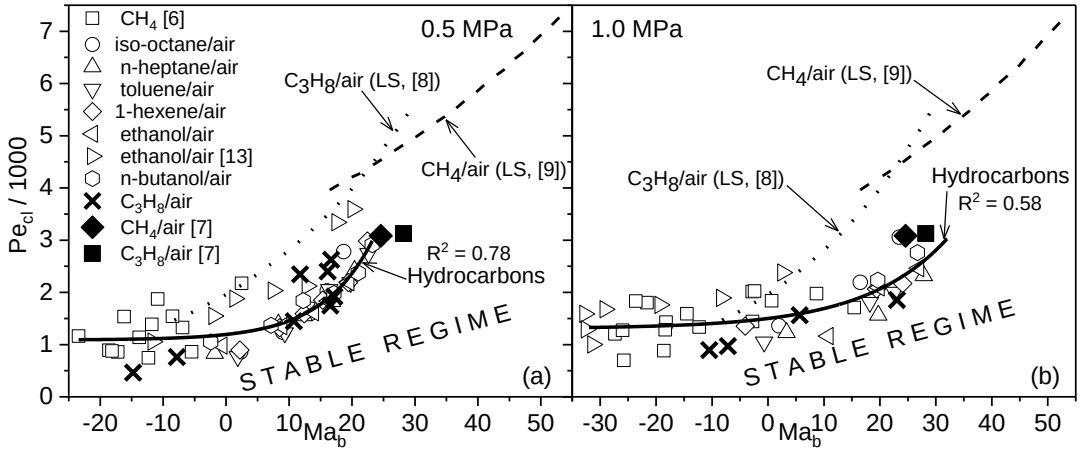

Figure 2. Pe_{cl} variations with Ma_b for different hydrocarbon/air explosion vessel data.

4. Results in terms of the critical Karlovitz number

Values of K_{cl} as a function of Ma_{sr} also were obtained from all the Pe_{cl}/Ma_b data in Figs. 1 and 2, using Eq. (3). These are re-presented in terms of plots of K_{cl} against Ma_{sr} for the separate fuels, in Fig. 3. Best fit curves are shown for high pressures explosions, all of which exhibit the same trend of more rapid increases in K_{cl} as Ma_{sr} is reduced. There is also a decrease in K_{cl} as the pressure is increased, indicative of generally improved flame stability. There are more data points at 0.5 and 1.0 MPa, a consequence of a reduction in δ_l with pressure, enabling the acquisition of more data for higher values of Pe_{cl}.

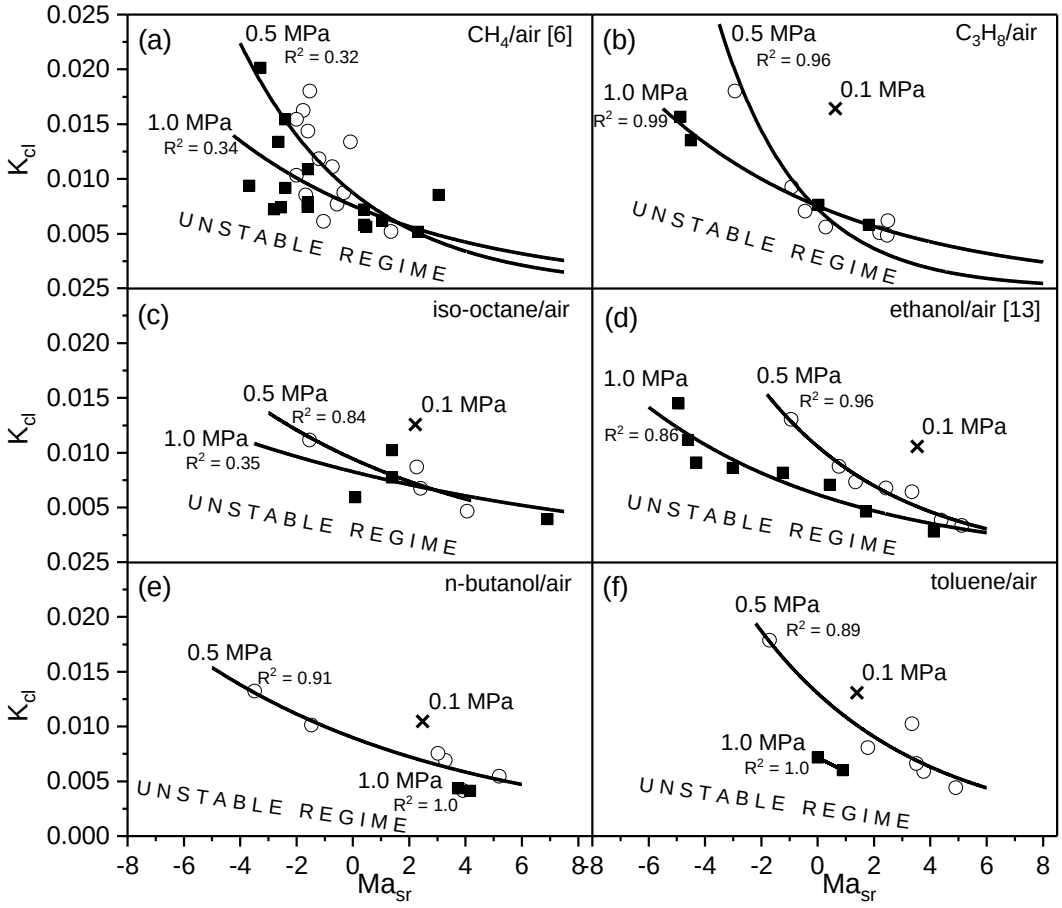

Figure 3. Values of K_{cl} plotted against Ma_{sr} for all hydrocarbon/air explosion vessel data.

There was no clear tendency for any fuel or group of fuels to exhibit a correlational trend comparable to that of pressure. In addition, any posible influence of σ was explored. It is significant, that the theory in [12] predicts it has a small influence on Pe_{cl}, particularly at the lower Markstein numbers. The present large data set was scrutinised and it revealed no such influence. This contrasts with other studies in which this variable was more successsfully isolated and controlled, such as the propane experiments in [20], and hydrogen experiments in [27].

All the hydrocarbon fuel data are plotted in terms of K_{cl} against Ma_{sr} for pressures of 0.1, 0.5 and 1.0 MPa in Fig. 4. The best fit expressions for these pressures are:

$K_{cl} = 0.015 \exp(-0.11 Ma_{sr})$ at 0.1 MPa, $R^2 = 0.95$. (5)

$K_{cl} = 0.009 \exp(-0.11 Ma_{sr})$ at 0.5 MPa, $R^2 = 0.58$. (6)

$K_{cl} = 0.007 \exp(0.11 Ma_{sr})$ at 1.0 MPa, $R^2 = 0.67$. (7)

Notwithstanding the scatter, there is a clear tendency for K_{cl} to decrease, and flames to become more stable, with increasing pressure.

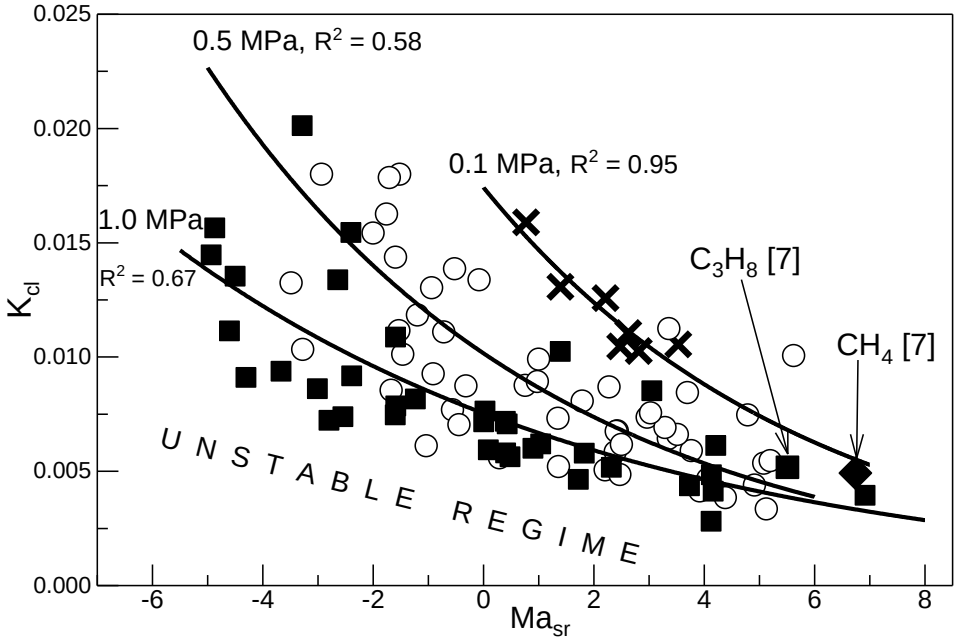

Figure 4. K_{cl} variations with Ma_{sr}. Explosion vessel data for different hydrocarbon/air mixtures at different pressures. Crosses (0.1 MPa), open circles (0.5 MPa), filled squares (1.0 MPa). Solid curves shows best fits through these data.

5. Discussion

Because of the key role of Pe_{cl}, the low values of both δ_l and flame radius in high pressure explosion vessels make it possible to predict the onset of instabilities in much larger explosions, at atmospheric pressure, P_a, from high pressure laboratory explosions, P. Figs. 3 and 4 clearly show the diverse influences of fuel, through values of Ma_{sr}, and pressure upon K_{cl}, and hence Pe_{cl}. These influences can be generalised to yield an expression for K_{cl} in terms of different values of P/P_a and Ma_{sr}. For all the hydrocarbons studied in the explosion vessel:

$$K_{cl} = 0.017.\exp(-0.165.Ma_{sr}).(P/P_a)^{-0.39}, \qquad R^2 = 0.66. \tag{8}$$

This relationship is shown by the bold curve in plot of $K_{cl}.(P/P_a)^{0.39}$ against Ma_{sr} in Fig. 5. The optimal relationships are also shown for 0.1, 0.5 and 1.0 MPa.

The large scale explosion data from LS [7] lie on the 0.1 MPa hydrocarbon curve. The LS C_3H_8 [8] and LS CH_4 [9] broken data curves are located somewhat further from the 0.1 MPa isobar. The asterisked points represent explosion vessel data for H_2/air at 0.1 MPa, and exhibit higher values of K_{cl}. The best curve fit through these data is shown by a thin solid line, which yields the expression:

$$K_{cl} = 0.0128.\exp(-0.32.Ma_{sr}). \quad (9)$$

These H_2 data were excluded from the earlier figures because of their wide divergence from the hydrocarbon data. The differences lie in the nature of correlations based on δ_l. Because H atoms diffuse rapidly in laminar flames towards the leading edge, where they initiate reaction to a greater extent than in hydrocarbon flames, the preheat zone is relatively much reduced [24, 25]. When hydrogen flame parameters are normalised by δ_l, there is a diminished comparability with other flames. An example is the normalising of jet flame diameters at blow-off with δ_l [26].

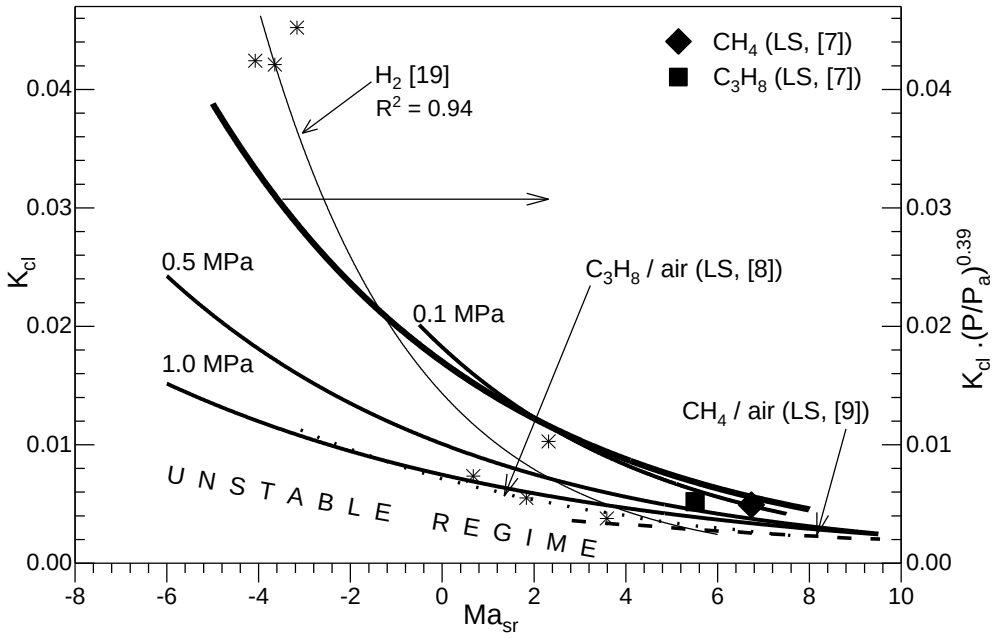

Figure 5. Solid curves show K_{cl} variations with Ma_{sr} from explosion vessel data at 0.1, 0.5 and 1.0 MPa alongside data for LS atmospheric explosions [7-9].

The large scale laminar atmospheric flames become unstable, with flame speeds that are predictable, using fractal approaches [3,4,7]. An important aspect of this is the pressure pulse generated by the accelerating flame.

The associated increasing rate of change of heat release rate generates appreciable pressure pulses [2]. In the large scale propane explosions of [7] the flame rapidly accelerated, with the flame speed more than tripling in 0.56 sec. Using the monopole assumption for the flame, it was estimated in [2] that, at a flame radius of 100 m, the maximum over-pressure one km from the propane fireball centre would be 0.3 kPa. A comparable atmospheric faster burning hydrogen flame, with ϕ = 0.5, would generate a significantly greater maximum over-pressure of 2 kPa. The reflection of such pressure pulses and their interactions with the flame can create Rayleigh-Taylor instabilities, additional to the existing instabilities, generating even stronger oscillatory pressure pulses [21].

An interesting aspect of flame instability is the practice of extrapolating a stable flame speed, or burning velocity, to zero stretch rate, using the observed stable relationship with stretch rate, to obtain a stretch free laminar burning velocity, notwithstanding such a value would reside in a regime of flame instability. Nevertheless, such values provide datums from which actual burning velocities can be derived, for given strain rates and curvatures, with the aid of the appropriate Markstein numbers.

Interestingly, in flames with only mild turbulence, there is a regime of enhanced turbulent burning velocity due to similar instabilities [22]. The maximum enhancement occurs at a turbulent Karlovitz stretch factor, K, of about 0.02, with negative Ma_{sr}.

6. Conclusions

(i). Analyses and experiments, involving explosions in a closed vessel, have identified the low strain rate regime in which laminar flames become unstable. The instabilities result in increasing flame wrinkling and burning velocities.

(ii). This approach makes it possible to predict flame speeds, consequent upon the release of flammable gas, under calm atmospheric conditions.

(iii). It also demonstrates how small laboratory explosions can be predictors of large atmospheric flame speeds.

(iv). It has been shown that large hydrogen atmospheric flame speeds deviate from the generalised expressions for hydrocarbons, and why this is so.

(v). The predictable atmospheric flame speed accelerations, due to increasing flame wrinkling, yield a rate of change of the heat release rate that creates a calculable overpressure. Such pressure pulses can further accelerate the flame due to Rayleigh-Taylor instabilities.

(vi). The increasing flame instabilities that occur as the critical Karlovitz number increases with decreasing Ma_{sr} is paralleled by a similar phenomenon in mildly turbulent flames.

(vii). In allowing for the effects of strain rate upon the laminar burning velocity of a mixture, it is not uncommon to postulate a laminar burning velocity at zero stretch rate. This is derived by extrapolating stable flame velocities at different strain rates to give a value at zero strain rate. Although convenient for correlations, in practice burning velocities would generally be higher due to instabilities.

ACKNOWLEDGEMENT

EPSRC and University of Leeds are thanked for the Research Scholarship Awards to Richard Mumby and Pervez Ahmed respectively.

REFERENCES

1. Bradley D., Lawes M., Mumby R., Cellular Flame Instabilities, Proceedings of the Eighth International Seminar on Fire and Explosion Hazards (ISFEH8), USTC Press, CHINA, 2016, pp. 579-587, Edited by Chao J., Liu N. A., Molkov V., Sunderland P., Tamanini F. and Torero J., DOI:10.20285/c.sklfs.8thISFEH.058 579.
2. Bradley, D., Dowling, A.P., Morgans, A.S., Combustion Instabilities, in Turbulent Premixed Flames, Eds. N. Swaminathan and K.N.C.Bray, Cambridge University Press., UK, 2011, pp. 151-243.
3. Gostintsev, Yu.A., Istratov, A.G., Shulenin, Yu.V., Combust. Explosion and Shock Waves March, (1988) 563–569. (Translated from FizikaGorenyiyaiVzryva 24(5)(1988) 63–70.
4. Bradley, D., Phil. Trans. R. Soc. London A357 (1999) 3567–3581.
5. Bradley, D., Hicks, R.A., Lawes, M., Sheppard, C.G.W., Woolley R., Combust. Flame115 (1998) 126–144.
6. Gu, X.J., Haq, M.Z., Lawes, M., Woolley, R., Combust. Flame 121 (2000) 41-58.
7. Bradley, D., Cresswell, T.M., Puttock, J.S., Combust. Flame. 124 (2001) 551-559.
8. Bauwens, C.R., Bergthorson, J.M., Dorofeev, S.B., Proc. Combust. Inst. 35 (2015) 2059-2066.

9. Regis, C., Bauwens, Bergthorson, Jeffrey M., Dorofeev, Sergey B., Critical Peclet Numbers for the onset of Darrieus-Landau Instability in Atmospheric-Pressure Methane-Air Flames, 25th ICDERS., University of Leeds (2015).
10. Kagan L., and Sivashinsky G. (2017), Proc. Combust. Inst., 36 (2017) 2709-2715.
11. Kagan L., and Sivashinsky G., Combust. Flame, 175 (2017) 307-311.
12. J.K. Bechtold, M. Matalon, Combust. Flame 67 (1987) 77-90.
13. Bradley, D., Lawes, M., Mansour, M.S., Combust. Flame. 156 (2009) 1462-1470.
14. Morley, C., "Gaseq: a chemical equilibrium program for Windows." http:// www. gaseq. co. uk. (2005).
15. Taylor, S.C., Burning velocity and the influence of flame stretch, PhD thesis, University of Leeds, 1991.
16. Bradley, D., Gaskell, P.H., Gu, X.J., Combust. Flame. 104 (1996) 176-198.
17. Bradley, D., Gaskell, P.H., Gu, X.J., Proc. Combust Inst. 27 (1998) 849-856.
18. Bradley, D., Sheppard, C. G. W., Woolley, R., Greenhalgh, D. A., Lockett, R. D., Combust. Flame 122 (2000) 195-209.
19. D. Bradley, M. Lawes, Kexin Liu, S. Verhelst, R. Woolley, Combustion and Flame 149 (2007) 162–172.
20. E. G. Groff, Combust. Flame 48 (1982) 51-62.
21. A. S. Al-Shahrany, D. Bradley, M. Lawes, K. Liu and R. Woolley, Combust. Sci. Tec., 178 (2006) 1771-1802.
22. Bradley, D., Lawes M., Kexin Liu, Mansour, M.S., Proc. Combust. Inst. 34 (2013) 1519–1526.
23. S. Verhelst, R. Woolley, M. Lawes, R. Sierens, Proceedings of the Combustion Institute 30 (2005) 209–216.
24. J. Gottgens, F. Mauss, N. Peters, Analytic approximations of burning velocities and flame thickness of lean hydrogen, methane, ethylene, ethane, acetylene and propane flames, Twenty-Fourth symposium (International) on Combustion/The Combustion Institute, 129-135 (1992).
25. D. Bradley, S. E-D. Habik, S.A, El-Sherif , Combust. Flame 87 (1991) 336-345.
26. Adriana Palacios, Derek Bradley, Combust. Flame 185, (2017) 309–318.
27. Sheng Yang, Abhishek Saha, Fujia Wu, Chung K. Law, Combustion and Flame 171 (2016), 112-118.